

On the route towards Si-based full color LED microdisplays for NTE applications

A. Smirnov

Laboratory of Information Displays and Optical Processing Systems, Belarusian State University of Informatics and Radioelectronics, Minsk 220027, Republic of Belarus

Tel. +375-17-2398858, smirnov@gw.bsuir.unibel.by

V. Labunov, S. Lazarouk

Laboratory of Nanotechnologies, Belarusian State University of Informatics and Radioelectronics, Minsk 220027, Republic of Belarus

Tel. +375-17-2020510, labunov@cit.org.by

Abstract

Design and manufacturing process of a full color LED microdisplay fabricated by standard CMOS technology and containing an array of aluminum / nanostructured porous silicon reverse biased light emitting Schottky diodes will be discussed. Being of a solid state construction, this microdisplays are cost-effective, thin and light in weight due to very simple device architecture. Its benefits include also super high resolution, wide viewing angles, fast response time and wide operating temperature range. The advantages of full integration of an LED-array and driving circuitry onto a Si-chip will be also discussed.

Key words: microdisplay, electroluminescence, inorganic materials

1. Introduction

A new very fast growing segment of electronic industry is the industry dealing with super miniature displays or microdisplays. They are finding the place in portable wireless communication devices, computing tools, digital still cameras, camcorders, advanced cell phones, and toys.

In principle, the simplest type of microdisplay is a light emitting device because it eliminates the need for an external light source and complicated optics, but their low luminance level limits their application to personal viewers. Most of the known light emissive technologies have been implemented as microdisplay technologies [1, 2].

In this presentation we will propose the alternative cost-effective approach based on the usage of Al / nanostructured porous silicon (NPS) reverse biased

light emitting Schottky diodes fabricated onto a silicon chip together with addressing ICs. The main advantages of such an approach are:

- 1). The usage of a simple and cost-effective standard bipolar semiconductor manufacturing process which provides full integration of addressing ICs with an array of Al / PS light emitting diodes and helps to integrate a lot of functionality into the display's silicon backplane;
- 2). Very high resolution and nanosecond response time of a Al/NPS LED microdisplay;
- 3). Low cost and simplicity of Al/NPS LED microdisplay fabrication, especially in the case of passive addressing.

2. State of the art

The first reversed biased PS LED was demonstrated by Richter et al. in 1991 [3]. A PS-layer was formed on a n-type silicon substrate following with the deposition of a semitransparent Au-electrode in order to form the Schottky structure. Light emission with the efficiency of 10^{-5} - 10^{-6} was observed in the visible range with the peak of 650 nm [4]. The lifetime of such devices varied from 45 min. to 100 h, after which the emission attenuation took place [5].

In 1995, we made a significant improvement in the efficiency and stability [6] through the formation of an oxidized PS layer protected from atmospheric oxygen by the additional passivation. The oxidized PS layer was formed on a low resistivity n-Si substrate by anodization in the transition regime [7], providing a continuous anodic oxide on the surface. Moreover, the additional passivation layer of a transparent anodic alumina Al_2O_3 was formed on the PS layer by a selective Al-anodization in an oxalic electrolyte during formation of an Al-Schottky electrode. It ensured the stability of continuous PS LED operation during 1000

h without visible degradation effects and increased quantum efficiency (10^{-3} - 10^{-4}) [8].

In 1998, V. Kuznetsov et al. [9] improved a PS LED design in order to enhance the device efficiency till 5×10^{-3} . In particular, they replaced the opaque electrode with a semitransparent silver electrode.

In 2000, the more efficient reverse biased PS LEDs have been reported by B. Gelloz et al. [10]. The quantum efficiency of about 10^{-2} has been obtained by using oxidized PS. Porous layer was formed on n⁺ silicon at 0°C. Then, the PS layer without drying was electrochemically oxidized by anodization in an aqueous solution of sulfuric acid. A Schottky barrier was formed by a transparent ITO deposition. The advancement of the anodization process by this way decreased the size of nonconfined silicon nanocrystals in PS. The enhanced quantum efficiency can be explained by the reduction of leakage carrier flow through the nonconfined silicon nanocrystals. Recently, the highest quantum efficiency of about 1.2×10^{-2} has been obtained by pulsed excitation [11]. Pulse LED operation allows one to reach the highest current density through a LED structure, which corresponds to maximum efficiency values.

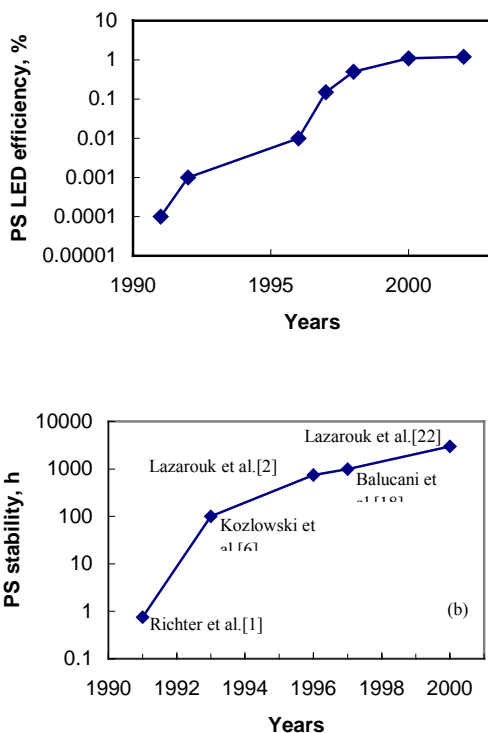


Fig.1. Efficiency (a) and stability (b) improvement of reverse biased PS LEDs.

Some common design ideas are present in all mentioned NPS LEDs:

- all are formed on n-type silicon substrates due to the higher Schottky barrier compared to p-type material;
- in addition, n⁺-silicon substrates are preferable because of minimal series resistance of PS LEDs;
- NPS must have homogeneous size distribution of nanocrystals over all the thickness and down to 1 μm. For this reason, oxidized PS was used in the device fabrication and the temperature of the PS formation was chosen to be 0°C;
- reverse biased LEDs have a nonlinear EL-I characteristics with an efficiency increasing with a current;
- optimized LED geometry and pulsed bias provide maximum LED current with the highest efficiency value;
- reverse biased PS LEDs can be formed also onto polysilicon [12] or amorphous silicon [13] layers as well as onto a transparent sapphire [14] or glass [15] substrates.

3. Al/NPS LED array fabrication process

The fabrication process and a NPS LED structure are shown in Fig.2. N-type single crystal silicon wafers with the resistivity of 4.5 Ω·cm were used as substrates in our experiments. High doped n⁺-silicon layer of about 100 nm thickness was formed on both sides of wafer by diffusion of phosphorous gas phase at a temperature of 950°C during 40 minutes (Fig. 2a). After doping treatment the surface resistivity of a sample was 10 Ω/□ (10^{20} dopant atoms/cm³). Then wafers were etched in hydrofluoric acid in order to remove the oxide formed during thermal treatment [16].

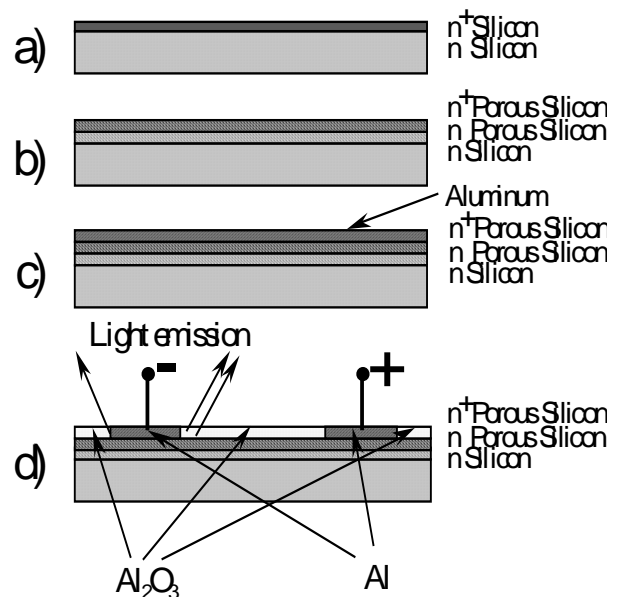


Fig.2. Schematic view of fabrication process and a PS LED structure: a) n^+ -type silicon wafer with n^+ -diffused layer; b) after anodization in transition regime, PS is formed both in n^+ -film and in a substrate layer; c) aluminum layer is deposited by magnetron sputtering; d) the final structure after photolithography and subsequent aluminum anodization. Light emission at the edge of negative biased pad is evidenced.

The PS layer was formed by anodization in transition regime, in 1% HF aqueous solution at $2-5 \text{ mA/cm}^2$. The thickness of PS film was higher than the n^+ -layer one, so that a thin layer of the n -substrate was also anodized (Fig. 2b).

To obtain metallic contact, $0.5 \mu\text{m}$ thick aluminum film was deposited by magnetron sputtering onto the porous layer (Fig. 2c). The Al electrodes (pads) were obtained by standard photolithography and subsequent

electrochemical aluminum anodization process. Aluminum anodization produced the transparent insulating alumina (Al_2O_3) areas between the aluminum pads so that light could be revealed (Fig. 2d).

The electrical contact on the wafer back side (not shown in the picture) was provided by the n^+ -diffused layer. Devices were biased connecting either two adjacent pads on the upper layer either one of the pads and the back side contact.

4. Experimental results

EL spectra

EL spectra were measured with the computer-aided spectrophotometer PEM-100, equipped with a cooled photomultiplier. PL spectra were measured under UV laser excitation at $\lambda=337 \text{ nm}$. The EL spectrum, measured in the $1.55-3.105 \text{ eV}$ energy range, for different currents through two adjacent electrodes are shown in Fig. 3.

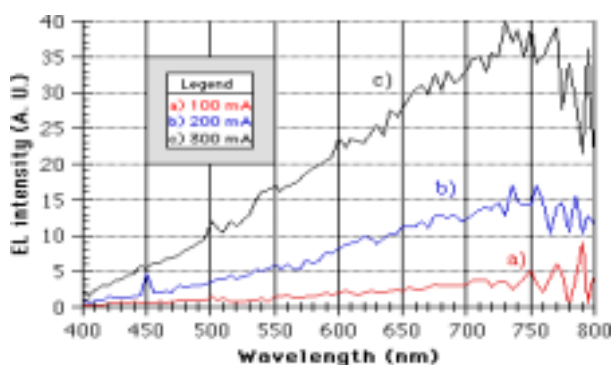


Fig. 3. EL spectrum for different currents through two adjacent electrodes at reverse bias.

Depending on PS anodizing regimes the emission peak can be both in the blue and in the red. But the emission spectra are very broad, with example which covers the whole visible range [17, 18]. The other approaches are to be used for a color microdisplays to get a narrow light emission spectra, say, the integration of a PS LED with a PS microcavity [19].

Response time


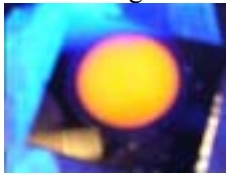

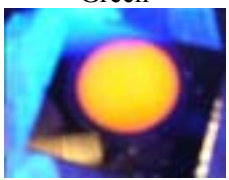
The shortest response time was published for forward biased PS LEDs [20]. However, our devices are faster, because they have no diffusion capacitance. The main mechanism of minor carrier generation in reverse biased Al/PS junctions is impact ionization at avalanche breakdown at high electric field. A regular columnar PS structure promotes the very fast avalanche breakdown due to non-uniform electric field distribution inside the PS layer [7]. The time of the avalanche response is estimated to be as less as 1 ps [21]. Thus, we have shown that our PS LEDs can operate in the nanosecond region. By further technology optimization, we hope to reach the sub-nanosecond range.

Colors

Initial wafers were boron doped silicon with resistivity of $12 \text{ Ohm}\cdot\text{cm}$. Anodizing processes were performed in aqueous-alcoholic solution HF (48%) : $\text{H}_2\text{O}:\text{C}_2\text{H}_5(\text{OH})=1:1:2$ electrolytes. Forming current densities were 20 mA/cm^2 for green and yellow photoluminescence, and 50 mA/cm^2 for the red ones. The anodizing time was 10-20 min. We used a postanodizing process to get the photoluminescent blue shift. During the postanodizing process the red PL transformed in orange and green PL. Samples were stood in an electrolyte in the dark condition during 10-35 minutes after the anodization.

Process regimes to get red, orange, yellow, and green photoluminescence are shown in a table 1.

Table 1. Manufacturing operation regimes for photoluminescence in various parts of the visible range

Photoluminescent samples	Anodizing regimes, j_f – forming current densities, t_f – anodizing time	Etching time in electrolyte after anodizing process, t_a
<p>Red</p> 	$j_f = 50 \text{ mA/sm}^2$ $t_f = 10 \text{ min}$	–
<p>Orange</p> 	$j_f = 20 \text{ mA/sm}^2$ $t_f = 20 \text{ min}$	$t_a = 10 \text{ min}$
<p>Yellow</p> 	$j_f = 20 \text{ mA/sm}^2$ $t_f = 20 \text{ min}$	$t_a = 15 \text{ min}$
<p>Green</p> 	$j_f = 20 \text{ mA/sm}^2$ $t_f = 20 \text{ min}$	$t_a = 30 \text{ min}$

Photoluminescent behaviour of different samples—without postanodizing treatment; standing in electrolyte during 20 minutes; standing in electrolyte during 30 minutes is shown in figure 4.

First, second, and third sample peak intensity wavelengths are 680 nm, 640 nm, and 580 nm, respectively. These peaks correspond to red, orange, and green optical ranges, respectively.

It was suggested in the very first reports on PS that the strong blue shift of the PL was caused by a quantum size effect, mainly due to the presence of quantum wires [25-29]. This effect results in the band gap widening of semiconductor materials.

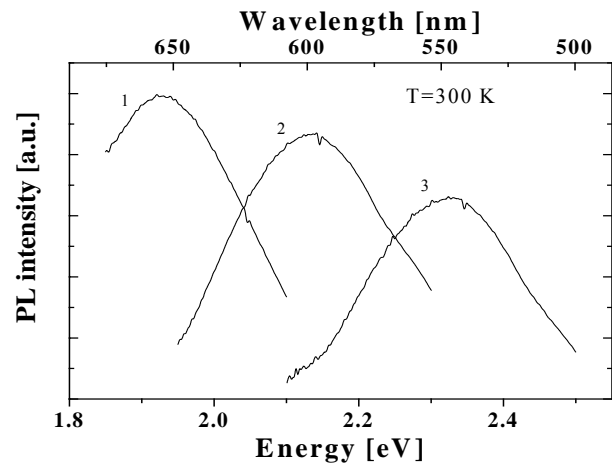


Fig. 4. PL spectra of NPS samples: 1 – without postanodizing treatment; 2 – standing in electrolyte during 20 minutes; 3 – standing in electrolyte during 30 minutes.

The PL blue shift can be explained by the size reduction of silicon nanoparticles during drying process. SiO_2 layer development reduces further silicon particle oxidizing, and results in increase of radiation wavelength stability.

Two models have been proposed to interpret the transition behavior based on the confinement effect. The first one is the band-to-band transition model [25]. And second one is the recombination-center-related transition model, involving surface states and disorder states [29]. However a basic lack of knowledge regards the ordering and the mean dimensionality and size dependence of these cores of freshly produced PS responsible for visible radiation from red to green.

5. Conclusions

The analysis of reverse biased Al/NPS LED developments for the last ten years has shown considerable parameter improvement towards practical implementations of these devices in microdisplay technology. Bright and stable light emission was observed in Al / NPS reverse biased Schottky junction. The time stability of light emission was quite high thanks to reliable passivation of porous silicon surface in the presented device construction.

Developed light emitting devices are totally compatible with modern silicon IC technology. Thus, Al/NPS light emitting structures fabricated onto a silicon chip containing driving circuitry can solve many miniaturization problems for microdisplay technologies.

This work is partly supported by ISTC grant B276-2.

6. References

- [1]. Allen K. A big-picture view of microdisplays, Seminar Lecture Notes, Boston, USA, May 2002, pp. M12/1-74.
- [2]. King C. History of TFEL technology at Planar System, Proc. Int. Conf. on Science and Technology of Emissive Displays and Lighting, Ghent, Belgium, September 2002, pp. 5-10.
- [3]. Richter A., Steiner P., Kozlowski F. and Lang W. Current-induced light emission from a porous silicon device, IEEE Electron Device Letters, 1991, No 12, pp. 691-693.
- [4]. Kozlowski F., Sauter M., Steiner P., Richter A., Sandmaier H., Lang W., Thin Solid Films, 1992, V. 222, pp. 196-199.
- [5]. Kozlowski F., Steiner P., Lang W., Proc. NATO ARW Series E: Applied Sciences, 1993, V. 244, pp. 123-133.
- [6]. Lazarouk S., Jaguiro P., Katsouba S., Masini, La Monica S., Maiello G., Ferrari A. Stable electroluminescence from reversed biased n - type porous silicon - aluminum Schottky junction device, Appl.Phys. Lett., 1996, V.68, pp. 2108-2110.
- [7]. Bertolotti M., Lazarouk S., Ferrari A. et al. Porous silicon obtained by anodization in the transition regime, Thin Solid Films, 1995, V.255, pp. 152-154.
- [8]. La Monica S., Lazarouk S. et al. Progress in the field of integrated optoelectronics based on porous silicon, Thin Solid Films, 1997, V. 297, pp. 261-264.
- [9]. Kuznetsov V., Andrienko I., Haneman D., Appl. Phys.Lett., 1998, V.72, pp. 3323-3325.
- [10]. Gelloz B., Koshida N., J.Appl.Phys., 2000, V.88, pp. 4319-4322.
- [11]. Lazarouk S., Smirnov A. , SPIE.- 2001.- June, V. 4511, pp. 68-71.
- [12]. Lazarouk S., Bondarenko V., La Monica S et al., Electroluminescence from Al/PS reverse biased Schottky diodes formed on the base of highly doped n-type polysilicon. Thin Solid Films, 1996, V. 276, pp. 296-299.
- [13]. Sercel P., Kwon D. et al., Visible electroluminescence from porous silicon/hydrogenated amorphous silicon pn - heterojunction devices, Appl. Phys. Lett., 1996, V.68, pp. 684-686.
- [14]. Lazarouk S. Light emitting devices based on Al / PS Schottky junctions on sapphire substrates for display applications, Proc. 7 ADT Symp., 1998, pp. 293-196.
- [15]. La Monica S., Lazarouk S. et al., Characterization of porous silicon light emitting diodes in high current density conditions, Solid State Phenomena, 1997, V. 54, pp. 21-26.
- [16]. Lazarouk S., Smirnov A., Labunov V. Fabrication of a full inorganic EL microdisplay integrated with addressing circuitry onto a Si - chip, Proc. Int. Conf. IDMC - 2003, Taipei, Taiwan, February 2003, pp. P3-08 - P3-11.
- [17]. Jaguiro P., Lazarouk S., Pavesi L., Smirnov A. Electroluminescence in porous silicon films of reverse biased Schottky junctions, Proc.ADT-2001, Minsk, Belarus, September 2001, pp. 112-115.
- [18]. Lazarouk S., Jaguiro P. et. al. Porous silicon light emitting diode and photodetector integrated with a multilayer alumina waveguide. Physics, Chemistry and Application of nanostructures, World Scientific, Singapore, 1999, pp. 370-373.
- [19]. Lazarouk S., Leshok A., Borisenko V. On the route towards Si-based optical interconnects, Microelectronic Eng., 2000, V.50, pp. 81-86.
- [20]. Cox T.I., Simmons A.J. et. al., J. Appl.Phys., 1999, V.86, pp. 2764-2773.
- [21]. Sze S. Semiconductor Devices: Physics and Technology, Bell Lab., A Wiley-Interscience publication, N.-Y., 1985.
- [22]. Lazarouk S., Smirnov A., Labunov V. et al. Inorganic EL microdisplay based on Al / porous silicon light emitting Schottky junctions, Eurodisplay - 2002 Proc., Nice, France, October 2002, pp. 683-684.
- [23]. Lazarouk S., Smirnov A., Labunov V. et al. Electroluminescent porous silicon microdisplay, EL-2002 Conference Proc., Ghent, Belgium, September 2002, pp. 391- 394.
- [24]. L. T. Canham, Appl. Phys. Lett. 57, 1046, 1990.
- [25]. S. Lazarouk, Proceeding of the 7th International Symposium "Advanced Display Technologies", December 1-5, 1998, pp 193-196.
- [26]. S. Lazarouk, P. Jaguiro, S. Katsouba, S. La Monica, G. Maiello, G. Masini, A. Ferrari, Thin Solid Film, vol. 68, 1996, pp. 2108-2110.
- [27]. Q. Zhang and S. C. Bayliss, J. Appl. Phys., 79, 1355, 1996.
- [28]. V. Lehmann and U. Gösele, Appl. Phys. Lett. 58, 856, 1991.
- [29]. J. M. Lavine, S. P. Sawan, Y. T. Shieh, and A. J. Bellezza, Appl. Phys. Lett. 62, 1099, 1993.